THE JOURNAL OF PHYSICAL CHEMISTRY B

ARTICLE

pubs.acs.org/JPCB

Membrane Activity of Tetra-*p*-guanidinoethylcalix[4]arene as a Possible Reason for Its Antibacterial Properties

Guillaume Sautrey,[†] Monika Orlof,[‡,†] Beata Korchowiec,[‡,†] Jean-Bernard Regnouf de Vains,[†] and Ewa Rogalska*[,†]

[†]Equipe GEVSM, Structure et Réactivité des Systèmes Moléculaires Complexes, UMR 7565 Nancy Université/CNRS, BP 239, 54506 Vandoeuvre-lès-Nancy cedex, France

[‡]Department of Physical Chemistry and Electrochemistry, Faculty of Chemistry, Jagiellonian University, R. Ingardena 3, 30-060 Krakow, Poland

ABSTRACT: Tetra-*p*-guanidinoethylcalix[4]arene trifluoroacetate salt (**CX1**) was synthesized recently as an antibacterial agent. It showed to be active in vitro against various Gram-positive and Gram-negative bacteria. To get more insight in the mechanism of the biological activity of this derivative, it was studied upon interactions with model lipid membranes. Langmuir monolayers were formed with zwitterionic 1,2-dimyristoyl-*sn*-glycero-3-phosphocholine or 1,2-dimyristoyl-*sn*-glycero-3-phosphoethanolamine, and with anionic 1,2-dimyristoyl-*sn*-glycero-3-phospho-*rac*-(1-glycerol) and 1,2-dimyristoyl-*sn*-glycero-3-phospho-L-serine. The two classes of lipids were used, respectively, as model lipids of the eukaryotic and bacterial cell membranes. The monolayers were exposed to **CX1** at different concentrations around the minimum inhibitory concentration found for *E. coli*. The surface pressure−area and surface potential−area compression isotherms, as well as Brewster angle microscopy and polarization-modulation infrared reflection−absorption spectroscopy, were employed to study the monolayers. The results obtained show a higher affinity of **CX1** for the anionic lipids, indicating importance of charge−charge interactions. On the basis of a comparative study of the behavior of **CX1** and that of *p*-guanidinoethylphenol trifluoroacetate salt, we propose that interplay of charge−charge and apolar interactions between **CX1** and lipids is responsible for the important reorganization of model membranes. This proposal may be helpful in developing new antibacterial calixarene derivatives.

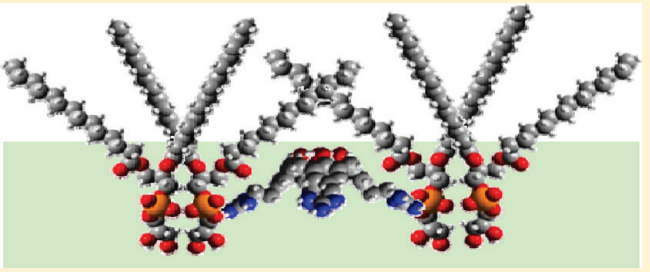

1. INTRODUCTION

New antibiotics are needed to combat the emergence of multidrug-resistant bacteria.[1−3] Most new antibiotics are obtained by improving the structure−activity relationship of the existing ones. One of the possible targets of new antibiotics is bacterial wall and, particularly, the bacterial phospholipid membrane, because the structure and chemical composition of the latter are common for a large number of species, but different compared to eukaryotic cells. It has been shown that the bacterial surface is negatively charged, due to the presence of teichoic acids in the plasma membrane of Gram-positive bacteria, lipopolysaccharides (LPS) in the outer membrane of Gram-negative bacteria, and a high proportion of anionic phospholipids such as phosphatidylglycerol (PG) in the phospholipidic membranes of both Gram-positive and Gram-negative bacteria.[4,5] On the contrary, the plasma membrane of mammalian cells, such as human cells, contains predominantly zwitterionic phospholipids such as phosphatidylcholines (PC) and sphingomyelins, as well as the neutral cholesterol. This lipid composition results in a net neutral charge of the mammalian cell membranes.[5] Consequently, a selective interaction and disruption of the bacterial membrane without toxicity for the eukaryotic host cells should be possible.[6,7]

It can be observed that the amphipathic, polycationic antimicrobial peptides (AMPs), in particular the arginine-rich peptides, which mode of action implies electrostatic and apolar interactions with negatively charged bacterial membranes and/or walls, induce membrane disruption and permeation;[7−13] the arginine-rich peptides indicate the importance of the cationic guanidinium moiety in their biological activity.[14−16] The guanidinium groups in AMPs can establish electrostatic and H-bonding interactions with biologically relevant phosphate groups[17] (Scheme 1A) acquiring defined spatial organization.[7,9,18] Interestingly, the guanidinium/phosphate associates are more stable at interfaces such as micelles, bilayers, and Langmuir monolayers compared to the molecular interface in bulk water.[19,20] Consequently, different synthetic, tailormade peptides were developed to better understand the relationship between their structure and bactericidal or endotoxin-neutralizing activity.[21−23]

Calixarene derivatives are of interest as possible bactericidal agents. Indeed, several calixarene derivatives with antimicrobial properties are described in the literature.[24] Recently, it was

Received: September 16, 2011
Revised: November 11, 2011
Published: November 14, 2011

dx.doi.org/10.1021/jp208970g | *J. Phys. Chem. B* 2011, 115, 15002–15012

Scheme 1. (A) Electrostatic and H-Bonding Interactions between Monosubstituted Guanidinium and Phosphodiester Groups,[20] and Structures of (B) Tetra-*p*-guanidinoethylcalix[4]arene Trifluoroacetate Salt (CX1) and (C) *p*-Guanidinoethylphenol Trifluoroacetate Salt (mCX1)

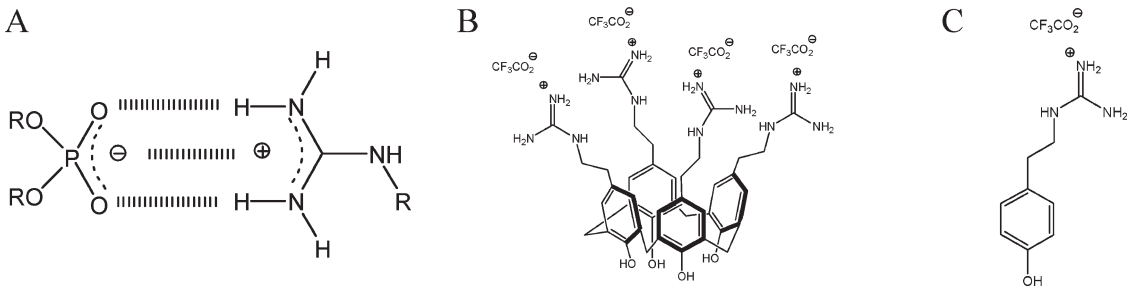

demonstrated that calixarene derivatives can be designed and synthesized to mimic the molecular dimensions and amphipathic surface topology of LPS-binding β-sheet and helical peptides. These novel sheet/helix topomimetics present hydrophobic and positively charged residues in a manner that allows some of them to effectively bind to and neutralize LPS endotoxin in vitro as well as in vivo. It was proposed that these agents may have utility in the clinic by providing a new means to combat LPS-induced endotoxemia and septic shock.[25]

In our group, several calix[4]arene derivatives were developed as bactericidal agents.[26] One of the amphipathic derivatives bearing *p*-guanidinoethyl groups, namely **CX1** (Scheme 1B), is active against different Gram-positive and Gram-negative bacteria; this derivative does not show cell toxicity.[27−29] The effects of **CX1** was disruption of the bacterial membrane,[30] modification of electrophoretic mobility,[30] and increased membrane permeability[31] in different bacterial strains. Interestingly, the activity of **CX1** showed to be significantly more important compared to the monomeric **mCX1** (Scheme 1C).

The results obtained are not unexpected. Indeed, our previous studies indicate that different calixarene derivatives are miscible with phosphoglycerides and can be easily incorporated into lipid membranes.[32] Moreover, the structure of the **CX1** derivative could be expected to favor the disruption of bacterial membranes according to the mode of action of different AMPs.[33] Many AMPs contain about 50% hydrophobic residues, together with a high number of cationic lysine and arginine residues, resulting in a net positive charge, the average net charge being +4.[13] A good balance between electrostatic and nonelectrostatic interactions, which is paramount for identifying AMPs of therapeutic interest[13] can be expected to be equally important in synthetic antimicrobial agents. The net charge +4 and the apolar calixarene crown make **CX1** a good candidate for studying the impact on model bacterial membranes.

In the present study, the Langmuir technique was used to gain a better understanding of the mechanism of the interactions of **CX1** with lipid membranes. Indeed, a phospholipid monolayer spread at the air−water interface can be considered as a half-membrane and used as a model of biological membranes.[34−36] These systems were used before to improve our understanding of the interactions between drugs and other molecules with model membranes.[16,37−41] Here, zwitterionic phospholipids, namely 1,2-dimyristoyl-*sn*-glycero-3-phosphocholine (DMPC) and 1,2-dimyristoyl-*sn*-glycero-3-phosphoethanolamine (DMPE), as well as anionic 1,2-dimyristoyl-*sn*-glycero-3-phospho-*rac*-(1-glycerol) (DMPG) and 1,2-dimyristoyl-*sn*-glycero-3-phospho-L-serine (DMPS) were used as model lipids of eukaryotic and bacterial cell membranes, respectively. The surface pressure−area ($\Pi-A$) and surface potential-area ($\Delta V-A$) compression isotherms, as well as Brewster angle microscopy (BAM) and polarization-modulation infrared reflection−absorption spectroscopy (PM-IRRAS), were employed to study the impact of **CX1** on the monolayers; the effect of **CX1** was compared with that of a monomeric compound, **mCX1**, bearing a single guanidinium group. The results obtained show a significant difference between the negatively charged and zwitterionic phosphoglycerides upon interaction with **CX1**. Indeed, the impact of **CX1** on model membranes is greater in the case of the negatively charged DMPG and DMPS compared to DMPC and DMPE bearing an overall neutral charge, and more important compared to **mCX1**. The lipids and the *p*-guanidinoethyl derivatives used in this study are depicted in Scheme 2.

2. EXPERIMENTAL SECTION

Chemicals. DMPC (99%), DMPE (99%), and DMPG (sodium salt 99%) were from Sigma. DMPS (sodium salt, 99%) was from Avanti Polar Lipids. Chloroform and methanol (both ~99.9% pure), used for preparing phospholipid solutions, were from Sigma-Aldrich. **CX1** (MW 1221.01) and **mCX1** (MW 293.24) were synthesized as described previously by M. Mourer et al.[26,27] The final white powders were obtained by lyophilization from aqueous solutions with high purity checked by NMR, mass spectrometry, and elemental analysis. **CX1** aqueous solutions, concentrations 0.4, 4.0, and 40.0 mg L^{-1} (0.3, 3.2, and 32.0 μM, respectively), were used as subphases; these concentrations were chosen because the minimum inhibitory concentration (MIC) found for **CX1** in *E. coli* is 4 mg L^{-1}.[28] An aqueous **mCX1** solution, concentration 3.8 mg L^{-1} (12.8 μM), was used as a blank; **mCX1** is not active against *E. coli* at this concentration. The overall molar concentration of guanidinium groups is 12.8 μM both in the case of **CX1**, concentration 4.0 mg L^{-1}, and in the case of **mCX1**, concentration 3.8 mg L^{-1}. **CX1** and **mCX1** do not aggregate in water at the concentrations used. The aqueous solutions were prepared with Milli-Q water, which had a surface tension of 72.8 mN m^{-1} at 20 °C (pH 5.6).

Compression Isotherms and Brewster Angle Microscopy. The surface pressure (Π) and electric surface potential (ΔV) measurements were carried out with a computer-interfaced KSV 2000 Langmuir balance coupled with a KSV Optrel BAM 300 Brewster angle microscope (KSV Instruments Ltd., Helsinki, Finland). The light source was a standard HeNe laser, 10 mW, 633 nm and the spatial resolution of the device is 2 μm. A Teflon trough (6.5 cm × 58 cm × 1 cm) with two hydrophilic Delrin

Scheme 2. Structures of the Molecules Used in This Study: (A) DMPC, (B) DMPE, (C) DMPG, (D) DMPS, (E) CX1, and (F) mCX1[a]

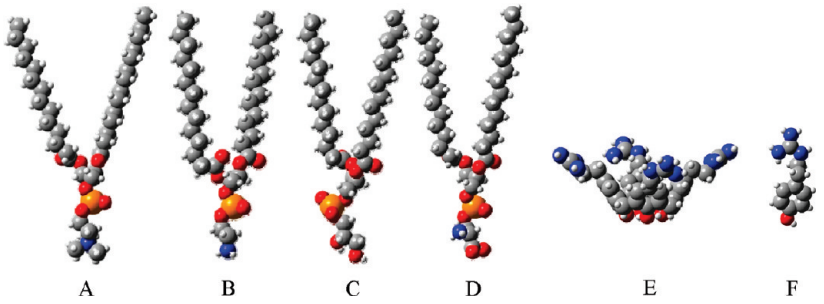

[a] The counterions were omitted for clarity. Color code: carbons in gray; oxygens in red; nitrogens in blue; phosphorous in orange; hydrogens in white. The structures of DMPC, DMPE, DMPG, DMPS, CX1, and mCX1 were obtained using GaussView 3.08.

barriers (symmetric compression) was used in compression isotherm experiments. The system was equipped with an electrobalance and a platinum Wilhelmy plate (perimeter 3.94 cm) as a surface pressure sensor. Surface potential was measured using a KSV Spot 1 with a vibrating plate electrode and a steel counter electrode immersed in the subphase. The apparatus was enclosed in a Plexiglas box, and temperature was kept constant at 20 °C. Before each run, the trough and the barriers were washed using cotton soaked in chloroform and ethanol and then with water and finally rinsed with Milli-Q water. The platinum Wilhelmy plate was cleaned between each experiment by rinsing with Milli-Q water, ethanol, and chloroform and heating to a red glow. All solvents used for cleaning the trough and the barriers were of analytical grade. Milli-Q water was used in all experiments. All impurities were removed from the subphase surface by sweeping and suction. When the surface pressure fluctuation was found to be lower than 0.2 mN m^{-1} during a compression stage, monolayers were spread at the air−water interface from calibrated solutions (concentration around 0.8 mg mL^{-1}) of DMPC in chloroform and DMPG, DMPE, and DMPS in chloroform/methanol mixture (3:1 v/v) using a microsyringe (Hamilton Co., USA). The stability of the surface potential signal was checked before each experiment, after the subphase surface was cleaned. After the ΔV signal had reached a constant value, it was zeroed, and the film was spread on the subphase. After the equilibration time of 15 min, the films were compressed at the rate of 5 mm min^{-1} by two symmetrically moving barriers. A PC computer and KSV software were used to control the experiments. Each compression isotherm was performed at least three times. The standard deviation was ±0.5 $Å^2$ for mean molecular area (A), ±0.2 mN m^{-1} for surface pressure (Π), and ±0.005 V for surface potential (ΔV) measurements. The compression isotherms allowed calculation of the compressibility modulus (C_s^{-1}; $C_s^{-1} = -A(\partial\Pi/\partial A)_T$).[42] The collapse parameters ΔV_{coll}, Π_{coll}, and A_{coll} were determined directly from the compression isotherms.

Adsorption Kinetics. The adsorption kinetics experiments were carried out with a computer-interfaced KSV 2000 Langmuir balance equipped with a Teflon trough (6.5 cm × 58 cm × 1 cm) kept at 20 °C. The monolayers were spread on pure water (330 mL) and compressed to a constant surface pressure of 30 mN m^{-1}. After an equilibration time of 10 min, 1.00 mL of calibrated aqueous solutions of **CX1** or **mCX1** (concentration around 1.25 mg mL^{-1}) was injected into the subphase using a microsyringe. The final concentration of guanidinium cations in the subphase was 12.8 μM with either derivative. The surface pressure versus time was monitored using a Langmuir balance.

Polarization-Modulation Infrared Reflection−Absorption Spectroscopy. The PM-IRRAS spectra of pure phospholipids spread on pure water, on 4.0 mg L^{-1} **CX1**, and on 3.8 mg L^{-1} **mCX1** solutions were registered at 20 °C. The Teflon trough dimensions were 36.5 cm (l) × 7.5 cm (w) × 0.5 cm (d); other experimental conditions were as described in the preceding paragraph. The PM-IRRAS measurements were performed using a KSV PMI 550 instrument (KSV Instruments Ltd., Helsinki, Finland). The PMI 550 contains a compact Fourier transform IR-spectrometer equipped with a polarization-modulation (PM) unit on one arm of a goniometer, and a MCT detector on the other arm. The incident angle of the light beam can be freely chosen between 40° and 90°; here, the incident angle was 75°. The spectrometer and the PM unit operate at different frequencies, allowing separation of the two signals at the detector. The PM unit consists of a photoelastic modulator (PEM), which is an IR-transparent ZnSe piezoelectric lens. The incoming light is continuously modulated between *s*- and *p*-polarization at a frequency of 74 kHz. This allows simultaneous measurement of spectra for the two polarizations, the difference providing surface specific information and the sum providing the reference spectrum. As the spectra are measured simultaneously, the effect of water vapor is largely removed. The PM-IRRAS spectra of the film-covered surface, $S(f)$, as well as that of the pure water, $S(w)$, were measured and the normalized difference $\Delta S/S = [S(f) - S(w)]/S(w)$ is reported. 6000 interferogram scans (10 scans per second) have been acquired for each spectrum. In the mid-IR region, the wavenumber at which the half-wave retardation takes place can be freely selected. Here, the maximum of PEM efficiency was set to either 1500 or 2900 cm^{-1} for analyzing the carbonyl, phosphate, or methylene stretching regions of the spectra, respectively. The spectral range of the device is 800−4000 cm^{-1} and the resolution is 8 cm^{-1}.

3. RESULTS AND DISCUSSION

Surface Pressure and Surface Potential Measurements. The $\Pi-A$ isotherms of phospholipid monolayers obtained in the absence and in the presence of **CX1** or **mCX1** are shown in Figure 1 (solid lines). The characteristic parameters of the isotherms are given in Tables 1 and 2. The effect of **mCX1** is observed only with the negatively charged lipids and, in particular, with DMPG (Figure 1C, magenta). The isotherms corresponding to

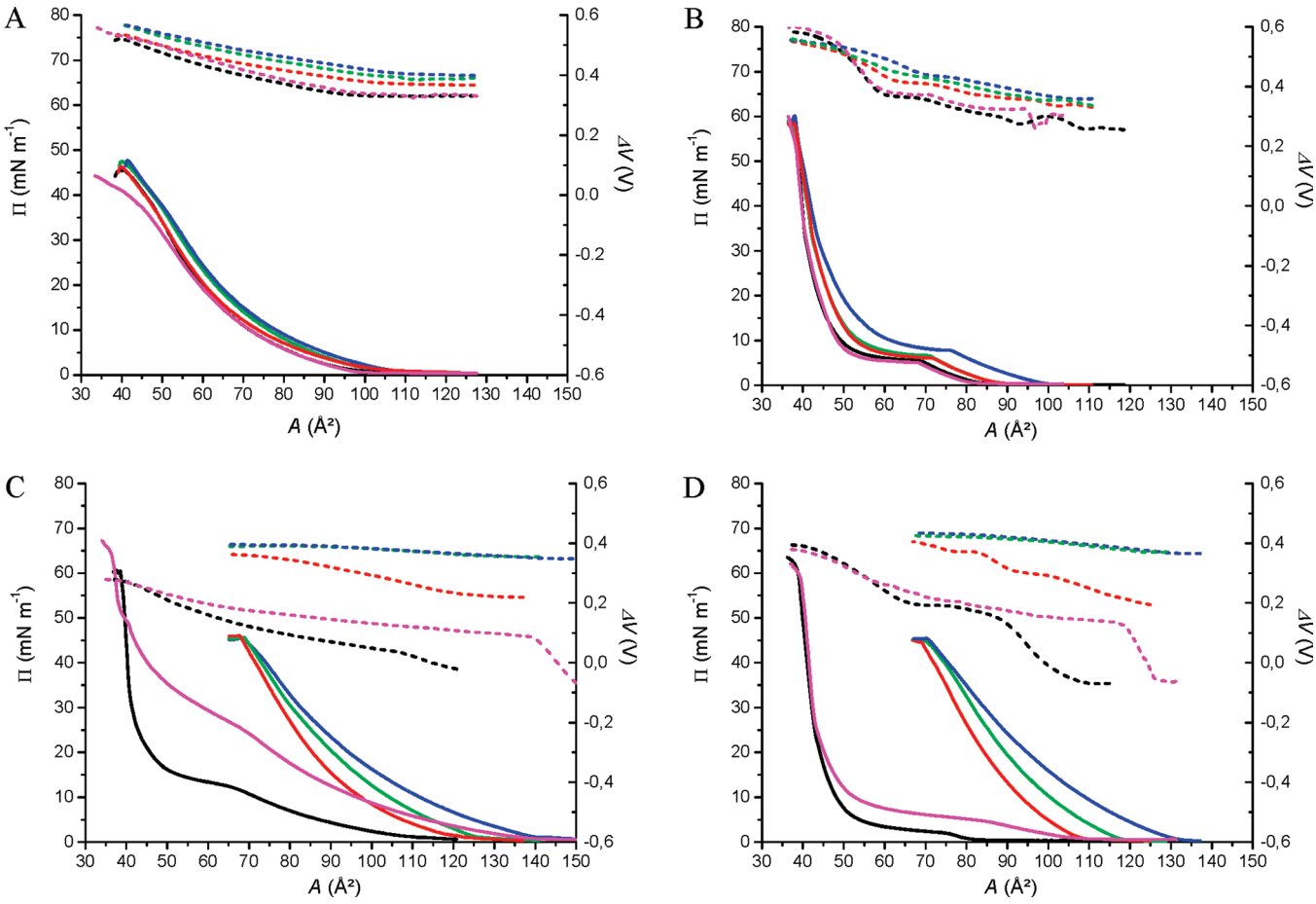

Figure 1. Compression isotherms of phospholipid monolayers spread on pure water and on **CX1** solutions: results obtained with (A) DMPC, (B) DMPE, (C) DMPG, and (D) DMPS. $\Pi-A$ isotherms, solid lines; $\Delta V-A$ isotherms, dotted lines. Phospholipid films spread on pure water (black); 0.4 mg L^{-1} **CX1** solution (red); 4.0 mg L^{-1} **CX1** solution (green); 40 mg L^{-1} **CX1** solution (blue); and 3.8 mg L^{-1} **mCX1** solution (magenta). Temperature: 20 °C.

the monolayers spread on subphases containing **CX1** are shifted to higher molecular areas compared to the pure water subphase. However, the shift is significantly more important in the case of the anionic DMPG and DMPS compared to the zwitterionic DMPC and DMPE. An important shift of the DMPG and DMPS $\Pi-A$ isotherms is observed already at 0.4 mg L^{-1} **CX1** subphase. Moreover, the liquid-expanded/liquid-condensed (LE/LC) phase transition observed in DMPG and DMPS spread on pure water disappears in the presence of 0.4 mg L^{-1} **CX1** in the subphase; the shift increases with the increasing concentrations of **CX1**. Furthermore, the stability of DMPG and DMPS films is greatly affected by the presence of **CX1** in the subphase, as indicated by the Π_{coll} values (Table 1). The decreasing values of Π_{coll} and the disappearance of the LE/LC phase transition show that the anionic films spread on subphases containing **CX1** are less stable and more liquidlike compared to the films spread on pure water.

The shift of the DMPG and DMPS $\Pi-A$ isotherms is comparable; with 0.4 mg L^{-1} **CX1** solution at the arbitrarily chosen surface pressure of 30 mN m^{-1} (Table 2) it is around 36 and 35 $Å^2$ for DMPG and DMPS, respectively, compared to water. This result suggests that a similar number of **CX1** molecules interacts with the DMPG and DMPS monolayers. The shifts at 30 mN m^{-1} for higher **CX1** concentrations are around 2.6 and 2.3 $Å^2$ for the DMPG and 3.9 and 2.7 $Å^2$ for DMPS isotherms, respectively. These observations indicate that at the concentration 0.4 mg L^{-1} the number of **CX1** molecules adsorbed on the negatively charged monolayers is close to saturation. It can be noted that **mCX1** is squeezed from the DMPS monolayer upon compression, but it is present even in the most condensed states of the DMPG monolayer. This result indicates that different types of interactions are established between **mCX1** and each of the two negatively charged lipids.

In the case of the zwitterionic phospholipids DMPC and DMPE, the difference between the $\Pi-A$ isotherms obtained on pure water and on **CX1** solutions is small, compared to DMPG and DMPS. At 30 mN m^{-1} the shift of the DMPC or DMPE isotherms corresponding to 40.0 mg L^{-1} **CX1** is around 3 $Å^2$ compared to pure water. The stability of the DMPC and DMPE monolayers in terms of Π_{coll} is not affected significantly by **CX1**. Moreover, the LE/LC phase transition is present in the DMPE monolayers for all **CX1** concentrations used. Overall, the surface pressure measurements show that modification of monolayer properties results from charge−charge interactions. Surface potential measurements (Figure 1, Tables 1 and 2) support the latter proposal, that is, higher affinity of **CX1** for anionic polar heads compared to zwitterionic polar heads. Indeed, the most important effect of **CX1** on the monolayers is observed with

Table 1. Isotherm Parameters at Collapse

	Π_{coll} (mN m^{-1})	A_{coll} (Å^2)	C_s^{-1} (mN m^{-1})	ΔV_{coll} (V)
DMPC on pure water	39.6	46.5	88.2	0.49
DMPC on 0.4 mg L^{-1}**CX1**	40.3	45.9	87.4	0.52
DMPC on 4.0 mg L^{-1}**CX1**	43.3	45.3	84.7	0.54
DMPC on 40 mg L^{-1}**CX1**	38.8	49.5	82.6	0.54
DMPC on 3.8 mg L^{-1}**mCX1**	37.0	45.8	80.4	0.51
DMPE on pure water	55.8	38.6	471.6	0.58
DMPE on 0.4 mg L^{-1}**CX1**	57.8	38.5	314.6	0.55
DMPE on 4.0 mg L^{-1}**CX1**	58.0	38.1	305.4	0.56
DMPE on 40 mg L^{-1}**CX1**	60.2	38.3	294.6	0.55
DMPE on 3.8 mg L^{-1}**mCX1**	54.0	38.5	413.8	0.60
DMPG on pure water	58.3	39.2	648.3	0.27
DMPG on 0.4 mg L^{-1}**CX1**	46.3	67.8	127.5	0.36
DMPG on 4.0 mg L^{-1}**CX1**	46.0	68.8	115.3	0.39
DMPG on 40 mg L^{-1}**CX1**	44.6	70.1	103.8	0.39
DMPG on 3.8 mg L^{-1}**mCX1**	63.4	36.9	416.5	0.28
DMPS on pure water	60.7	39.0	424.6	0.39
DMPS on 0.4 mg L^{-1}**CX1**	44.6	69.4	147.1	0.40
DMPS on 4.0 mg L^{-1}**CX1**	43.2	72.3	129.3	0.42
DMPS on 40 mg L^{-1}**CX1**	45.7	70.6	98.8	0.43
DMPS on 3.8 mg L^{-1}**mCX1**	59.0	39.8	494.5	0.38

Table 2. Isotherm Parameters at 30 mN m^{-1}

	A (Å^2)	C_s^{-1} (mN m^{-1})	ΔV (V)
DMPC on pure water	52.5	85.8	0.46
DMPC on 0.4 mg L^{-1}**CX1**	52.7	81.6	0.49
DMPC on 4.0 mg L^{-1}**CX1**	54.9	76.5	0.51
DMPC on 40 mg L^{-1}**CX1**	55.8	78.5	0.52
DMPC on 3.8 mg L^{-1}**mCX1**	51.2	67.4	0.49
DMPE on pure water	41.2	194.7	0.58
DMPE on 0.4 mg L^{-1}**CX1**	43.2	162.5	0.53
DMPE on 4.0 mg L^{-1}**CX1**	43.2	153.6	0.54
DMPE on 40 mg L^{-1}**CX1**	44.6	114.6	0.54
DMPE on 3.8 mg L^{-1}**mCX1**	41.4	191.7	0.59
DMPG on pure water	41.7	181.8	0.26
DMPG on 0.4 mg L^{-1}**CX1**	78.0	117.3	0.35
DMPG on 4.0 mg L^{-1}**CX1**	80.5	95.5	0.39
DMPG on 40 mg L^{-1}**CX1**	82.6	75.8	0.39
DMPG on 3.8 mg L^{-1}**mCX1**	58.8	27.5	0.20
DMPS on pure water	42.2	366.7	0.38
DMPS on 0.4 mg L^{-1}**CX1**	77.8	126.4	0.37
DMPS on 4.0 mg L^{-1}**CX1**	81.7	125.3	0.42
DMPS on 40 mg L^{-1}**CX1**	84.4	89.4	0.43
DMPS on 3.8 mg L^{-1}**mCX1**	42.5	376.6	0.37

DMPG (Tables 1 and 2). The increase of the ΔV values in the presence of **CX1** in the subphase may be related to dehydration of the PG headgroups; this effect is less important in the case of DMPS containing multiple intramolecular hydrogen bonds.[43] By the same token, the effect of dehydration can be observed in DMPC containing a higher amount of highly coordinated water population, compared to DMPE in which more disorder in the hydrogen-bonding network of water around the headgroup was observed.[44]

Microbiological studies using fluorescent labeling showed modification of membrane permeability in bacteria exposed to **CX1**.[31] The permeability properties of biological membranes can be correlated with monolayer compressibility.[38−40] The latter property is quantified using compressibility modulus,[42] C_s^{-1}, calculated from the $\Pi-A$ isotherms. As shown in Table 1, the values of C_s^{-1} decrease with the increasing concentration of **CX1** in the subphase. The liquefaction of the monolayers is significant for the negatively charged DMPG, followed by DMPS. In the case of the zwitterionic DMPE the liquefaction effect is low, and still lower in the case of DMPC.

It was shown previously in our group that **mCX1**, contrary to **CX1**, has no significant antibacterial activity.[27,28] Here, the impact of the two compounds on the model membranes was compared at the same molar concentrations of the guanidinium groups present in the two compounds (Figure 1, Tables 1 and 2). The concentration used was 12.8 μM, which is 4.0 mg L^{-1} of **CX1** or 3.8 mg L^{-1} of **mCX1**. It can be observed that **mCX1** (Figure 1, magenta curves) does not modify the properties of the phospholipid monolayers as significantly, as **CX1** does (Figure 1, green curves).

To compare the impact of **CX1** and **mCX1** on the lipid monolayers, adsorption experiments were performed (Figure 2). Concentrated aqueous solutions of **CX1** or **mCX1** were injected into the pure water subphase (final concentration of guanidinium cations 12.8 μM) under the phospholipid monolayers compressed to an initial surface pressure Π = 30 mN m^{-1}. In the case of **CX1**, a rapid increase of surface pressure was observed with the negatively charged DMPG and DMPS. In the case of **mCX1**, surface pressure increased somewhat with the monolayer formed with DMPG. These results show that **CX1** penetrates from the subphase into the negatively charged monolayers at the surface pressure considered as equivalent to the pressure in biological membranes.[45]

We propose that both charge−charge and apolar interactions are responsible for the observed effects. Indeed, it can be imagined that, upon adsorption of **CX1** to the negatively charged monolayers, interactions between the guanidinium groups and the negatively charged polar heads of DMPG or DMPS are established, followed by accommodation of the calixarene crown in the apolar part of the monolayer. This effect would be facilitated by the fact that the hydrophilicity of the hydroxyl groups in **CX1** is low due to an intramolecular H-bond network. In the case of **mCX1** the charge−charge interactions allow adsorption to the negatively charged monolayers. However, squeezing out from the monolayer is observed at around 25 mN m^{-1} in the case of **mCX1** and DMPS (Figure 1D, solid magenta curve). We propose that this effect is due to the absence of apolar interactions stabilizing **mCX1** in the monolayer. We propose also that hydrogen bonding established between the hydroxyl moiety in **mCX1** and those present in the polar headgroup of DMPG may stabilize **mCX1** in the monolayer formed with the latter lipid. Indeed, **mCX1** is not squeezed from this film even at high condensation states (Figure 1C, solid magenta curve) and, on the other hand, it penetrates into the DMPG monolayer at Π = 30 mN m^{-1} (Figure 2B, green curve).

The analysis of the compression isotherms of negatively charged lipids indicates that Gibbs energy (ΔG) of the penetration process is negative in the case of **CX1**. In the case of **mCX1** the absolute value of ΔG is lower and, at high surface pressures, ΔG is positive. The **CX1** penetration is probably enthalpy controlled due to formation of more than one ion−ion interaction per molecule, in spite of a high entropy cost of introducing **CX1** into the layer.

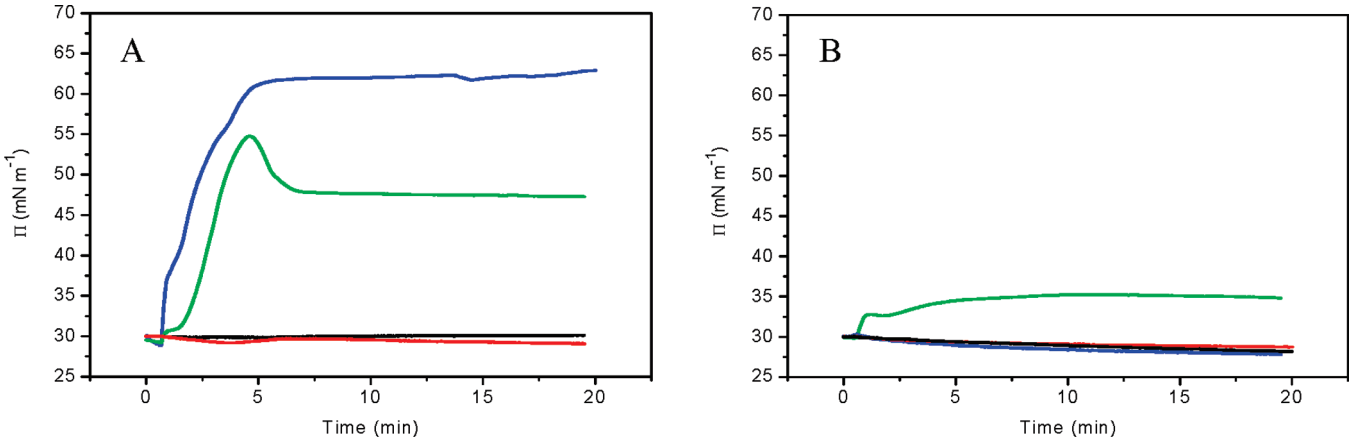

Figure 2. Adsorption kinetics of **CX1** (A) and **mCX1** (B) to phospholipid monolayers compressed at an initial surface pressure Π = 30 mN m^{-1}. DMPC, black; DMPE, red; DMPG, green; DMPS, blue. Final concentration of **CX1** and **mCX1** in the subphase: 4.0 mg L^{-1} (12.8 μM of guanidinium cations) and 3.8 mg L^{-1} (12.8 μM of guanidinium cations), respectively. Temperature: 20 °C.

In other words, in the case of **CX1**, entropy of penetration is not balanced by exothermic ionic interactions. It can be expected that **mCX1** penetration to the layer is entropy controlled.

Brewster Angle Microscopy (BAM). To gain more insight into the morphology of phospholipid monolayers upon interactions with **CX1**, BAM measurements were performed. Because DMPE and DMPG monolayers form characteristic domains in the LE/LC phase transition region, these lipids were used in the experiments as zwitterionic and anionic model lipids, respectively. The BAM images of pure DMPE or DMPG monolayers spread on pure water as well as on the 4.0 mg L^{-1} **CX1** or 3.8 mg L^{-1} **mCX1** solutions are presented in Figure 3. The snapshots taken at 6.0, 7.0, and 9.5 mN m^{-1} show the LE/LC phase transition of the DMPE monolayer spread on pure water (A−C), on the **CX1** solution (D−F) and on the **mCX1** solution (G−I). The snapshots (J−L) and (M−O) show the LE/LC phase transition in DMPG monolayers spread on pure water and the **mCX1** solution, respectively, at the molecular area values of 68, 60, and 48 Å^2. As indicated by the corresponding Π−*A* isotherm (Figure 1), the DMPG monolayers spread on **CX1** solution do not show phase transition. The corresponding BAM images were uniformly black, which confirmed the isotropy of the film (images not shown).

On the other hand, the morphology of domains formed in the LE/LC phase transition of the DMPG monolayer spread on pure water or **mCX1** solution are compared at constant area, because of an important difference of the phase transition surface pressures observed with the two subphases.

In the case of DMPE, the condensed-phase domains are clearly visible in the films formed on all subphases (Figure 3A−I). The condensed-phase domains observed in the presence of **CX1** in the subphase (Figure 3D−F) are smaller compared to pure water (Figure 3A−C). On the contrary, the condensed domains formed in the presence of **mCX1** in the subphase (Figure 3G−I) are bigger compared to those formed on the pure water subphase (Figure 3A−C). In general, the morphology of the DMPE monolayer is not significantly affected by **CX1** or **mCX1** present in the subphase.

More significant effect of **CX1** and **mCX1** is observed in the DMPG films (Figure 3J−O). The condensed-phase domains observed in the LE/LC phase transition of DMPG monolayer spread on pure water (Figure 3J−L) disappear in the presence of **CX1** in the subphase and the film shows isotropy, as indicated by the uniformly gray images (results not shown). This suggests that the liquefaction of the DMPG film in the presence of **CX1** is more pronounced than for DMPE. In the case of DMPG monolayer spread on the **mCX1** subphase (Figure 3M−O), condensed-phase domains are clearly visible in the LE/LC phase transition. However, these domains are smaller and more numerous compared to pure water, which suggests liquefaction of the DMPG monolayer formed on the **mCX1** solution. However, this effect is less pronounced compared to **CX1**, for which the LE/LC phase transition disappears. It can be concluded that the results obtained with BAM are in accordance with the analysis of the compression isotherms and support our observations that the impact of **CX1** on monolayers is significantly more important compared to **mCX1**.

Polarization-Modulation InfraRed Reflection−Absorption Spectroscopy (PM-IRRAS). In order to better understand the bonding mode of **CX1** and **mCX1** to lipids, PM-IRRAS experiments[46−48] were performed. The PM-IRRAS spectra of pure phospholipid monolayers obtained in the absence and in the presence of **CX1** (4.0 mg L^{-1}) or **mCX1** (3.8 mg L^{-1}) are shown in Figure 4. Characteristic vibration bands of phospholipids are reported in Table 3. All spectra were collected at the surface pressure of 30 mN m^{-1}, which is the density range considered as representative for biological membrane.[45] The effect of **CX1** or **mCX1** on the hydrophobic region of monolayers, such as alkyl chains, can be monitored via the frequencies of asymmetric and symmetric stretching vibrations of methylene groups $\nu_{as}(CH_2)$ and $\nu_s(CH_2)$, around 2920 and 2850 cm^{-1}, respectively. Moreover, the effect of **CX1** or **mCX1** on the polar heads of lipids can be monitored via the frequencies of the stretching vibration of carbonyl moieties ν(C═O) and the asymmetric stretching vibration of phosphate moieties $\nu_{as}(PO_2^-)$, around 1730 and 1220 cm^{-1}, respectively. The frequencies of $\nu_{as}(CH_2)$ and $\nu_s(CH_2)$ are sensitive to the conformation of phospholipid alkyl chains,[49,50] while the frequencies of ν(C═O) and $\nu_{as}(PO_2^-)$ are sensitive to the hydration state of phospholipid polar heads.[51,52]

A shift of $\nu_{as}(CH_2)$ and $\nu_s(CH_2)$ to lower wavenumbers (red shift) indicates alkyl chains ordering in the monolayer, while a shift to higher wavenumbers (blue shift) results from chains disordering and an increase of conformational liberty.[53,54] The stretching

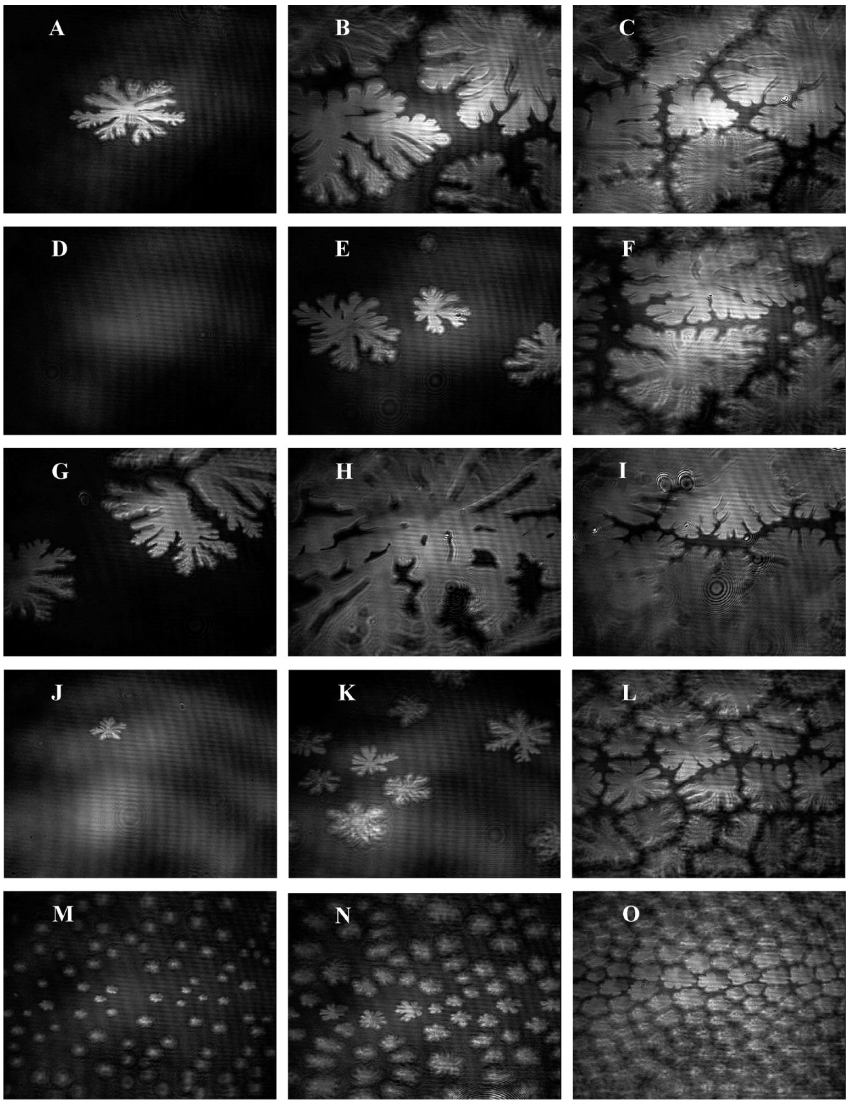

Figure 3. BAM micrographs of DMPE (A−I) and DMPG (J−O) monolayers. Line A−C: DMPE on pure water at 6.0 (A), 7.0 (B), and 9.5 (C) mN m^{-1}. Line D−F: DMPE on 4.0 mg L^{-1} **CX1** solution at 6.0 (D), 7.0 (E), and 9.5 (F) mN m^{-1}. Line G−I: DMPE on 3.8 mg L^{-1} **mCX1** solution at 6.0 (G), 7.0 (H), and 9.5 (I) mN m^{-1}. Line J−L: DMPG on pure water at 66 (J), 60 (K), and 48 $Å^2$ (L). Line M−O: DMPG on 3.8 mg L^{-1} **mCX1** solution at 66 (M), 60 (N), and 48 $Å^2$ (O). Scale: the width of the snapshots corresponds to 345 μm. Temperature: 20 °C.

bands ν(C═O) and $\nu_{as}(PO_2^-)$ are sensitive to H-bonding and, consequently, to the hydration state of the polar heads. A shift to lower wavenumbers indicates hydration, while a shift to higher wavenumbers indicates dehydration of the corresponding group due to decrease of water accessibility.[52,55]

The $\nu_{as}(CH_2)$ and $\nu_s(CH_2)$ values obtained at 30 mN m^{-1} for the films spread on pure water (Table 3) are in accordance with compressibility calculations (Table 2). Indeed, the highest chain ordering that is the lowest $\nu_{as}(CH_2)$ and $\nu_s(CH_2)$ values as well as the highest C_s^{-1} correspond to DMPS; DMPC chains are the least ordered among the four lipids, while DMPE and DMPG are intermediary in this respect.

The ν(C═O) stretching band values, lower in the zwitterionic phospholipids compared to the negatively charged indicate a higher hydration of the former (Table 3).[56] This effect may be due to the sodium counterion present in the negatively charged headgroups. The interference of the counterion with the carbonyl groups could decrease their water accessibility.[57,58]

On the contrary, the $\nu_{as}(PO_2^-)$ vibrations (Table 3) show that the phosphate groups are more hydrated in the negatively charged phospholipids DMPG and DMPS, compared to DMPC and DMPE. It can be supposed that the interactions between the phosphate anion and the choline or the ethanolamine cations decrease the water accessibility of the phosphate moiety.[59]

The presence of **CX1** (4.0 mg L^{-1}; 12.8 μM guanidinium group concentration) in the subphase induces a shift of the $\nu_{as}(CH_2)$ and $\nu_s(CH_2)$ bands to higher wavenumbers in the case of DMPG and DMPS, indicating disordering of the phospholipid alkyl chains that is a more liquidlike character of the monolayers. No significant effects of **CX1** on the carbonyl hydration of zwitterionic lipids are observed, particularly in the case of DMPC. A small shift (4 cm^{-1}) in the ν(C═O) band of DMPE to higher wavenumbers can be noticed, indicating a minor dehydration the carbonyl moieties. However, for both DMPG and DMPS, important shifts of the ν(C═O) band in the presence of **CX1** are visible. The deconvolution of the spectra reveals two peaks,

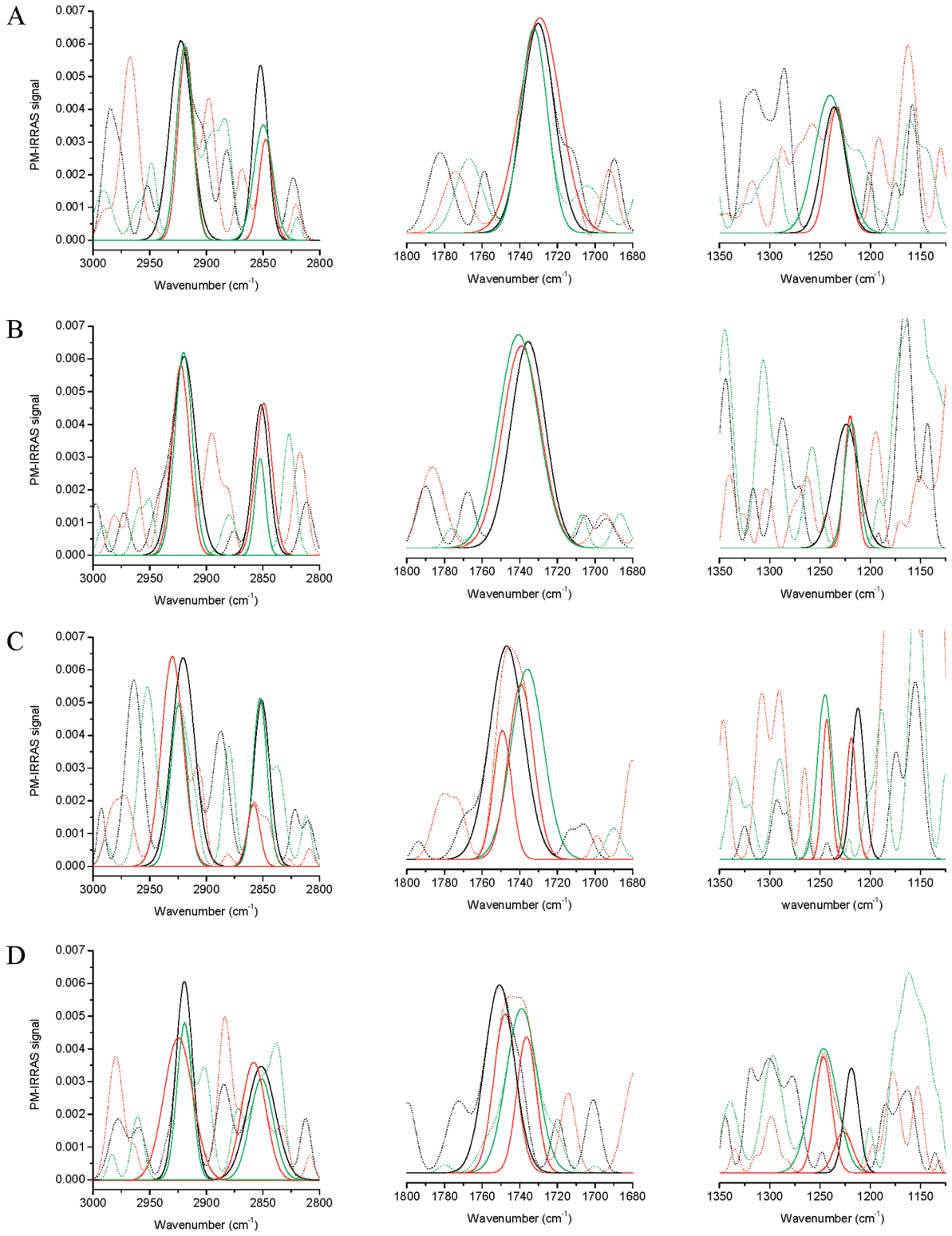

Figure 4. PM-IRRAS spectra, collected at Π = 30 mN m^{-1}, in the spectral regions of methylene (left column), carbonyl (middle column), and phosphate (right column) stretching vibrations. Results obtained with DMPC (line A), DMPE (line B), DMPG (line C), and DMPS (line D). Phospholipid films spread on pure water (black); 4.0 mg L^{-1} **CX1** solution (red); and 3.8 mg L^{-1} **mCX1** solution (green). Temperature 20 °C.

which were assigned to the *sn*-1 and *sn*-2 carbonyl groups. This split of the ν(C═O) band may be, indeed, due to a restricted conformational liberty of the ester moieties and a differentiating chemical environment of the *sn*-1 and *sn*-2 carbonyl groups.[58,60] This effect of **CX1** could be brought about by changes in the conformation of the glycerol backbone.[58] The peak at the higher value was attributed to the *sn*-1 carbonyl group, whereas the peak at the lower value to the *sn*-2 carbonyl group.[52,58]

The *sn*-1 carbonyl groups are slightly dehydrated in DMPG and slightly hydrated in DMPS as shown, respectively, by the blue and red shift of the corresponding band (2 and 3 cm^{-1} for DMPG and DMPS, respectively), while the *sn*-2 carbonyl groups are strongly hydrated in both cases, as shown by the red shift of the second band (8 cm^{-1}), compared to the single band observed with the pure water subphase. This indicates that the chemical environment of the *sn*-1 carbonyl groups is not significantly modified in the presence of **CX1**. Nevertheless, the water accessibility of the *sn*-2 carbonyl groups increases. This could be due to displacement of the Na^+ cation from the polar head to the subphase, and to binding of the guanidinium groups to the anionic phosphate moiety in the lipids. The interaction between the phosphodiester anion and a guanidinium cation involves hydrogen bonding and is highly directional.[61,62] In consequence, a specific conformation of the lipid polar heads can be induced by the adsorption of **CX1** to anionic monolayers.

The interactions of **CX1** with the negatively charged polar heads show in the shifts of the ν(C═O) bands. However, it can be supposed that the **CX1** guanidinium groups bind to the anionic phosphate groups in the lipids. To clarify this point, the $\nu_{as}(PO_2^-)$ region was investigated in PM-IRRAS (Figure 4). It can be observed that, in the case of DMPG and DMPS, the $\nu_{as}(PO_2^-)$ vibration is significantly affected by the presence of **CX1**. Indeed, the $\nu_{as}(PO_2^-)$ signal is split in two bands; both are shifted to higher wavenumbers. These two $\nu_{as}(PO_2^-)$ bands suggests a coexistence of two populations of phosphate groups. It is reasonable to suppose that binding of the guanidinium moieties to the phosphate groups by strong and directional interactions[61,62] involving electrostatic interactions and H-bonding[63,64] induces dehydration of the phosphate moiety.[65] Consequently, the strongly blue-shifted peak can be attributed to lipids bound with **CX1** via phosphate/guanidinium interaction;[66] the peak showing at the lower, weakly blue-shifted value can be attributed to unbound lipids. In the case of DMPC or DMPE, the cationic choline or ethanolamine groups in the polar heads can be expected to hinder the guanidinium/phosphate interaction.[67]

The effects of **mCX1** are clearly seen with the negatively charged DMPG and DMPS (Figure 4, green curves). In the presence of **mCX1** (3.8 mg L^{-1}; 12.8 μM guanidinium group concentration) in the subphase the $\nu_{as}(PO_2^-)$ band in DMPG and DMPS are strongly shifted to higher wavenumbers (Table 3). The shift is comparable with the more blue-shifted $\nu_{as}(PO_2^-)$ band observed in the presence of **CX1** in the subphase, indicating dehydration of the phosphate groups. Obviously, this effect is due to **mCX1** bonding to the anionic lipids. The presence of a single

Table 3. Methylene, Carbonyl, and Phosphate Stretching Vibrations of Pure Phospholipids in the Absence and in the Presence of CX1 or mCX1 (Π = 30 mN m^{-1})

	$\nu_{as}(CH_2)$ (cm^{-1})	$\nu_s(CH_2)$ (cm^{-1})	ν(C═O) (cm^{-1})	$\nu_{as}(PO_2^-)$ (cm^{-1})
DMPC on pure water	2923	2852	1730	1236
DMPC on 4.0 mg L^{-1} **CX1**	2918	2848	1729	1233
DMPC on 3.8 mg L^{-1} **mCX1**	2919	2850	1733	1240
DMPE on pure water	2920	2852	1735	1224
DMPE on 4.0 mg L^{-1} **CX1**	2922	2850	1739	1220
DMPE on 3.8 mg L^{-1} **mCX1**	2920	2852	1741	1219
DMPG on pure water	2920	2851	1747	1212
DMPG on 4.0 mg L^{-1} **CX1**	2930	2858	1739, 1749	1219, 1243
DMPG on 3.8 mg L^{-1} **mCX1**	2924	2853	1736	1245
DMPS on pure water	2919	2850	1751	1219
DMPS on 4.0 mg L^{-1} **CX1**	2925	2858	1736, 1748	1226, 1246
DMPS on 3.8 mg L^{-1} **mCX1**	2919	2851	1739	1246

Scheme 3. A Proposal of Interactions between DMPG and CX1 or mCX1 in Monolayers Spread at the Air−Water Interface. (A) mCX1 Intercalated between the Polar Heads of DMPG; Side View. (B) CX1 Bound to Two DMPG Molecules via Polar and Apolar Interactions and Two Unbound DMPG Molecules; Side View. (C) CX1 with Two Bound and Two Unbound DMPG Molecules; Top View[a]

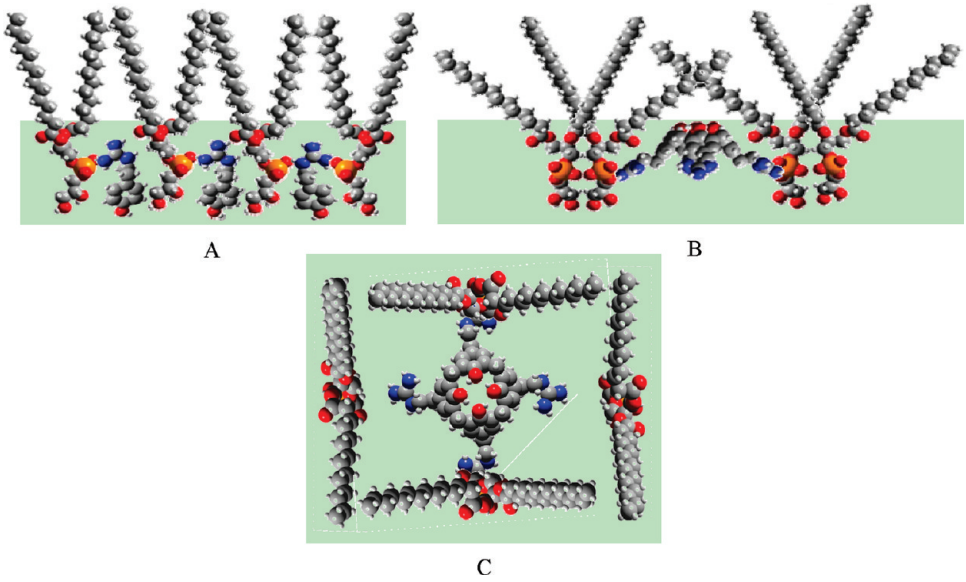

[a] Counterions were omitted, for clarity. Color code: carbons in gray; oxygens in red; nitrogens in blue; phosphorous in orange; hydrogens in white; water subphase in green. The structures of DMPC, DMPE, DMPG, DMPS, CX1, and mCX1 were obtained using GaussView 3.08.

$\nu_{as}(PO_2^-)$ peak suggests that all lipids interact with **mCX1**. Interestingly, the single $\nu(C{=}O)$ band corresponding to the carbonyl moieties in DMPG and DMPS is shifted to lower wavenumbers, indicating hydration of the carbonyl groups; this effect can be due to the displacement of the Na^+ cations from the polar heads to the subphase. Finally, the effect of **mCX1** in the subphase shows as a small blue shift of the $\nu_{as}(CH_2)$ and $\nu_s(CH_2)$ bands in DMPG and DMPS (Table 3). The fact that **mCX1** interacts with phosphate moieties without affecting the conformations of the hydrocarbon chains indicates that this molecule does not penetrate into the apolar part of the monolayer. Overall, our results indicate that **mCX1** interacts with the lipid layers via polar interactions (Scheme 3A). Indeed, this derivative can establish charge−charge interactions with the phosphate group. On the other hand, the phenolic hydroxyl group is available for hydrogen bonding. In the case of DMPG, the hydrogen bonding with the hydroxyl groups present in the polar head may be the reason for a more stable interaction with the monolayer compared to DMPS. In the case of **CX1** (Scheme 3B,C), interactions between four phospholipid molecules can be envisaged, via four guanidinium groups. However, due to steric hindrance, a negative cooperativity of charge−charge interactions between **CX1** and the phospholipids may be expected; this possible effect is graphically schematized in Scheme 3C. Splitting of the $\nu(C{=}O)$ and $\nu_{as}(PO_2^-)$ signals observed in the PM-IRRAS spectra, indicating coexistence of two distinct lipid populations, namely one which interacts and another one which does not interact with **CX1**, supports this proposal. The resulting heterogeneity of the membrane composition may be responsible for the important liquefaction of the DMPS and DMPG monolayers observed in the presence of **CX1**. It can be supposed that the same effect is responsible for the fragilization of bacterial membranes observed in vitro. We propose that stabilization of the **CX1**−phospholipid adducts involves the oppositely charged groups that is guanidinium cations in **CX1** and phosphate anions in the phospholipids, as well as the interactions between the apolar moieties in **CX1** and in the lipid. These interactions are schematically depicted in Scheme 3B.

4. CONCLUSIONS

This work shows that the trifluoroacetate salts of **CX1** and **mCX1**, while featuring some common structural characteristics, have different impact on model lipid membranes. The effects of these positively charged molecules are clearly seen in the case of the negatively charged phospholipids, namely DMPG and DMPS; no significant modification of the properties of the monolayers formed with the zwitterionic DMPC and DMPE was observed. This discrimination between the two classes of phosphoglycerides indicates that charge−charge attraction plays a decisive role in the interactions between the model membranes and the two guanidinoethyl derivatives. However, the two derivatives behave differently with the negatively charged membranes. Indeed, all physicochemical properties of the DMPG and DMPS films are modified to a much greater degree by **CX1** compared to **mCX1**. Moreover, the fact that **mCX1** is expelled from the DMPS film upon compression indicates that the system it forms with the lipid layer is less stable compared to **CX1**. The overall results indicate that stability of the **CX1**−lipid layer is due to both charge−charge and apolar interactions; the latter are absent in the case of **mCX1**. Formation of stable **CX1**−lipid complexes coexisting with unbound lipids may be one cause of bacterial membrane fragility and possible disruption, and of the subsequent antibacterial activity observed in the case of **CX1**, but not in the case of **mCX1**.

AUTHOR INFORMATION

Corresponding Author

*E-mail: ewa.rogalska@srsmc.uhp-nancy.fr. Tel.: +33 (0)3 83 68 43 45. Fax: +33 (0)3 83 68 43 22.

ACKNOWLEDGMENT

G.S. acknowledges Ministère de l'Education Nationale, de l'Enseignement Supérieur et de la Recherche, France, and M.O. the Ministry of Science and Higher Education, Poland, for their Ph.D. fellowships. Discussions with Dr. Jacek Korchowiec are highly appreciated. The authors thank Dr. J. Korchowiec for preparing the models of the molecules used in this study. We thank Eric Dubs and Francis Hoffmann for their excellent technical assistance.

REFERENCES

(1) Hancock, R. E. W.; Knowles, D. *Curr. Opin. Microbiol.* **1998**, *1*, 493–494.
(2) Leeb, M. *Nature* **2004**, *431*, 892–893.
(3) Hurdle, J. G.; O'Neill, A. J.; Chopra, I.; Lee, R. E. *Nat. Rev. Microbiol.* **2011**, *9*, 62–75.
(4) Brock, T. D. *Biology of Microorganisms*, 2nd ed.; Prentice-Hall: Upper Saddle River, NJ, 1974.
(5) Verkleij, A. J.; Zwal, F. A.; Roelofsen, B.; Comfurius, P.; Kastelijn, D.; Van Deenen, L. L. M. *Biochim. Biophys. Acta, Biomembr.* **1973**, *323*, 178–193.
(6) Kratzer, C.; Tobudic, S.; Graninger, W.; Buxbaum, A.; Georgopoulos, A. *J. Hosp. Infect.* **2006**, *63*, 316–322.
(7) Matsuzaki, K. *Biochim. Biophys. Acta, Biomembr.* **1999**, *1462*, 1–10.
(8) Shai, Y. *Biochim. Biophys. Acta, Biomembr.* **1999**, *1462*, 55–70.
(9) Epand, R. M.; Vogel, H. J. *Biochim. Biophys. Acta, Biomembr.* **1999**, *1462*, 11–28.
(10) Volinsky, R.; Kolusheva, S.; Berman, A.; Jelinek, R. *Biochim. Biophys. Acta, Biomembr.* **2006**, *1758*, 1393–1407.
(11) Godballe, T.; Nilsson, L. L.; Petersen, P. D.; Jenssen, H. *Chem. Biol. Drug Des.* **2011**, *77*, 107–116.
(12) Vaara, M. *Curr. Opin. Pharmacol.* **2009**, *9*, 571–576.
(13) Stroemstedt, A. A.; Ringstad, L.; Schmidtchen, A.; Malmsten, M. *Curr. Opin. Colloid Interface Sci.* **2010**, *15*, 467–478.
(14) Strom, M. B.; Rekdal, O.; Svendsen, J. S. *J. Pept. Sci.* **2002**, *8*, 431–437.
(15) Lehrer, R. I.; Barton, A.; Daher, K. A.; Harwig, S. S. L.; Ganz, T.; Selsted, M. E. *J. Clin. Invest.* **1989**, *84*, 553–561.
(16) Barzyk, W.; Campagna, S.; Wieclaw, K.; Korchowiec, B.; Rogalska, E. *Colloids Surf. A* **2009**, *343*, 104–110.
(17) Springs, B.; Haake, P. *Bioorg. Chem.* **1977**, *6*, 181–190.
(18) Wu, M.; Hancock, R. E. W. *J. Biol. Chem.* **1999**, *274*, 29–35.
(19) Onda, M.; Yoshihara, K.; Koyano, H.; Ariga, K.; Kunitake, T. *J. Am. Chem. Soc.* **1996**, *118*, 8524–8530.
(20) Ariga, K.; Kunitake, T. *Acc. Chem. Res.* **1998**, *31*, 371–378.
(21) Mayo, K. H.; Ilyina, E.; Park, H. *Protein Sci.* **1996**, *5*, 1301–1315.
(22) Mayo, K. H.; Haseman, J.; Ilyina, E.; Gray, B. *Biochim. Biophys. Acta, Gen. Subjects* **1998**, *1425*, 81–92.
(23) Mayo, K. H.; Haseman, J.; Young, H. C.; Mayo, J. W. *Biochem. J.* **2000**, *349*, 717–728.
(24) Lamartine, R.; Tsukada, M.; Wilson, D.; Shirata, A. *C. R. Chim.* **2002**, *5*, 163–169.

(25) Chen, X.; Dings, R. P. M.; Nesmelova, I.; Debbert, S.; Haseman, J. R.; Maxwell, J.; Hoye, T. R.; Mayo, K. H. *J. Med. Chem.* **2006**, *49*, 7754–7765.
(26) Mourer, M.; Dibama, H. M.; Fontanay, S.; Grare, M.; Duval, R. E.; Finance, C.; Regnouf-de-Vains, J.-B. *Bioorg. Med. Chem.* **2009**, *17*, 5496–5509.
(27) Mourer, M.; Duval, R. E.; Finance, C.; Regnouf-de-Vains, J.-B. *Bioorg. Med. Chem. Lett.* **2006**, *16*, 2960–2963.
(28) Grare, M.; Mourer, M.; Fontanay, S.; Regnouf-de-Vains, J.-B.; Finance, C.; Duval, R. E. *J. Antimicrob. Chemother.* **2007**, *60*, 575–581.
(29) Grare, M.; Massimba Dibama, H.; Lafosse, S.; Ribon, A.; Mourer, M.; Regnouf-de-Vains, J.-B.; Finance, C.; Duval, R. E. *Clin. Microbiol. Infect.* **2010**, *16*, 432–438.
(30) Grare, M.; Dague, E.; Mourer, M.; Regnouf-de-Vains, J.-B.; Finance, C.; Duval, J. F. L.; Duval, R. E.; Gaboriaud, F. *Pathol. Biol.* **2007**, *55*, 465–471.
(31) Grare, M.; Fontanay, S.; Massimba Dibama, H.; Mourer, M.; Regnouf-de-Vains, J.-B.; Finance, C.; Duval, R. E. *Pathol. Biol.* **2010**, *58*, 46–51.
(32) Korchowiec, B.; Ben Salem, A.; Corvis, Y.; Regnouf de Vains, J.-B.; Korchowiec, J.; Rogalska, E. *J. Phys. Chem. B* **2007**, *111*, 13231–13242.
(33) Brogden, K. A. *Nat. Rev. Microbiol.* **2005**, *3*, 238–250.
(34) Brezesinski, G.; Mohwald, H. *Adv. Colloid Interface Sci.* **2003**, *100−102*, 563–584.
(35) Korchowiec, B.; Korchowiec, J.; Hato, M.; Rogalska, E. *Biochim. Biophys. Acta, Biomembr.* **2011**, *1808*, 2466–2476.
(36) Korchowiec, B.; Paluch, M.; Corvis, Y.; Rogalska, E. *Chem. Phys. Lipids* **2006**, *144*, 127–136.
(37) Korchowiec, B.; Ben Salem, A.; Corvis, Y.; Regnouf de Vains, J.-B.; Korchowiec, J.; Rogalska, E. *J. Phys. Chem. B* **2007**, *111*, 13231–13242.
(38) Czapla, K.; Korchowiec, B.; Orlof, M.; Magnieto, J. R.; Rogalska, E. *J. Phys. Chem. B* **2011**, *115*, 9290–9298.
(39) Gravier, J.; Korchowiec, B.; Schneider, R.; Rogalska, E. *Chem. Phys. Lipids* **2009**, *158*, 102–109.
(40) Wieclaw, K.; Korchowiec, B.; Corvis, Y.; Korchowiec, J.; Guermouche, H.; Rogalska, E. *Langmuir* **2009**, *25*, 1417–1426.
(41) Corvis, Y.; Barzyk, W.; Brezesinski, G.; Mrabet, N.; Badis, M.; Hecht, S.; Rogalska, E. *Langmuir* **2006**, *22*, 7701–7711.
(42) Davies, J. T.; Rideal, E. K. *Interfacial Phenomena*, 2nd ed.; Academic Press: London, 1963.
(43) Mukhopadhyay, P.; Monticelli, L.; Tieleman, D. P. *Biophys. J.* **2004**, *86*, 1601–1609.
(44) Watry, M. R.; Tarbuck, T. L.; Richmond, G. L. *J. Phys. Chem. B* **2003**, *107*, 512–518.
(45) Blume, A. *Biochim. Biophys. Acta, Biomembr.* **1979**, *557*, 32–44.
(46) Blaudez, D.; Buffeteau, T.; Cornut, J. C.; Desbat, B.; Escafre, N.; Pezolet, M.; Turlet, J. M. *Appl. Spectrosc.* **1993**, *47*, 869–874.
(47) Blaudez, D.; Buffeteau, T.; Cornut, J. C.; Desbat, B.; Escafre, N.; Pezolet, M.; Turlet, J. M. *Thin Solid Films* **1994**, *242*, 146–150.
(48) Blaudez, D.; Turlet, J.-M.; Dufourcq, J.; Bard, D.; Buffeteau, T.; Desbat, B. *J. Chem. Soc., Faraday Trans.* **1996**, *92*, 525–530.
(49) Dicko, A.; Bourque, H.; Pezolet, M. *Chem. Phys. Lipids* **1998**, *96*, 125–139.
(50) Pinazo, A.; Wen, X.; Liao, Y.-C.; Prosser, A. J.; Franses, E. I. *Langmuir* **2002**, *18*, 8888–8896.
(51) Cornut, I.; Desbat, B.; Turlet, J. M.; Dufourcq, J. *Biophys. J.* **1996**, *70*, 305–312.
(52) Hubner, W.; Blume, A. *Chem. Phys. Lipids* **1998**, *96*, 99–123.
(53) Dyck, M.; Kerth, A.; Blume, A.; Loesche, M. *J. Phys. Chem. B* **2006**, *110*, 22152–22159.
(54) Bi, X.; Flach, C. R.; Perez-Gil, J.; Plasencia, I.; Andreu, D.; Oliveira, E.; Mendelsohn, R. *Biochemistry* **2002**, *41*, 8385–8395.
(55) Allouche, M.; Castano, S.; Colin, D.; Desbat, B.; Kerfelec, B. *Biochemistry* **2007**, *46*, 15188–15197.
(56) Czapla, K.; Korchowiec, B.; Rogalska, E. *Langmuir* **2010**, *26*, 3485–3492.
(57) Korchowiec, B.; Orlof, M.; Sautrey, G.; Ben Salem, A.; Korchowiec, J.; Regnouf-de-Vains, J.-B.; Rogalska, E. *J. Phys. Chem. B* **2010**, *114*, 10427–10435.
(58) Casal, H. L.; Mantsch, H. H.; Hauser, H. *Biochemistry* **1987**, *26*, 4408–4416.
(59) Lafrance, D.; Marion, D.; Pezolet, M. *Biochemistry* **1990**, *29*, 4592–4599.
(60) Binder, H.; Kohler, G.; Arnold, K.; Zschornig, O. *Phys. Chem. Chem. Phys.* **2000**, *2*, 4615–4623.
(61) Schug, K. A.; Lindner, W. *Chem. Rev. (Washington, DC, United States)* **2005**, *105*, 67–113.
(62) Hauser, S. L.; Johanson, E. W.; Green, H. P.; Smith, P. J. *Org. Lett.* **2000**, *2*, 3575–3578.
(63) Janout, V.; Jing, B.; Staina, I. V.; Regen, S. L. *J. Am. Chem. Soc.* **2003**, *125*, 4436–4437.
(64) Sakai, N.; Matile, S. *J. Am. Chem. Soc.* **2003**, *125*, 14348–14356.
(65) Li, S.; Su, Y.; Luo, W.; Hong, M. *J. Phys. Chem. B* **2010**, *114*, 4063–4069.
(66) Adams, J. M.; Small, R. W. H. *Acta Crystallogr., Sect. B: Struct. Sci.* **1976**, *B32*, 832–835.
(67) Tang, M.; Waring, A. J.; Hong, M. *J. Am. Chem. Soc.* **2007**, *129*, 11438–11446.